

Constraining Theories of SiO Maser Polarization: Analysis of a $\pi/2$ EVPA Change

T. L. Tobin^{1,2}, A. J. Kemball¹ and M. D. Gray²

¹Department of Astronomy, University of Illinois at Urbana-Champaign
1002 W. Green Street, Champaign, IL 61801, USA

²Jodrell Bank Centre for Astrophysics, Alan Turing Building, University of Manchester
Manchester M13 9PL, UK

Abstract. The full theory of polarized SiO maser emission from the near-circumstellar environment of Asymptotic Giant Branch stars has been the subject of debate, with theories ranging from classical Zeeman origins to predominantly non-Zeeman anisotropic excitation or propagation effects. Features with an internal electric vector position angle (EVPA) rotation of $\sim \pi/2$ offer unique constraints on theoretical models. In this work, results are presented for one such feature that persisted across five epochs of SiO $\nu = 1, J = 1 - 0$ VLBA observations of TX Cam. We examine the fit to the predicted dependence of linear polarization and EVPA on angle (θ) between the line of sight and the magnetic field against theoretical models. We also present results on the dependence of m_c on θ and their theoretical implications. Finally, we discuss potential causes of the observed differences, and continuing work.

Keywords. masers, polarization, magnetic fields, stars: AGB and post-AGB

1. Introduction

Although theories have endeavored to explain the polarization of SiO masers originating from the near circumstellar environments (NCSE) of Asymptotic Giant Branch (AGB) stars, no theoretical consensus has yet been reached. Prominent theories as to the origin of SiO $\nu = 1, J = 1 - 0$ maser polarization ascribe it to the local magnetic field (Goldreich *et al.* 1973, Elitzur 1996) or a change in the anisotropy of pumping radiation conditions or other non-Zeeman effects (Asensio Ramos *et al.* 2005, Watson 2009).

However, these theories differ in their ability to explain rotations of the EVPA by $\sim \pi/2$ within a single maser feature. In some theories, such as Goldreich *et al.* (1973) (hereafter GKK), the Electric Vector Position Angle (EVPA) is governed by the angle, θ , between the magnetic field and the line of sight. When θ is small, the linear polarization would be parallel to the projected magnetic field. However, when θ becomes larger than the Van Vleck angle ($\sim 55^\circ$), the polarization would be perpendicular to the projected magnetic field. In this case, a rotation of the EVPA across a feature could be due to a slight change in the direction of the magnetic field with respect to the line of sight, spanning the Van Vleck angle.

This rotation could also be due to a change in the direction of the projected magnetic field across the spatial extent of the maser feature in the image plane. In this case, the EVPA would again be defined by the direction of the projected magnetic field in the sky, but the angle of the projected magnetic field would rotate within the masing material (Soker & Clayton 1999).

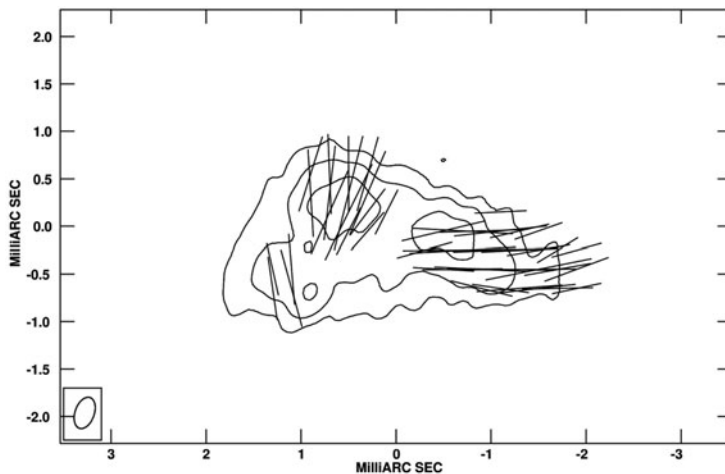


Figure 1. Target maser feature in epoch BD46AO. Contours denote frequency-averaged Stokes I with levels of $\{-10, -5, 5, 10, 20, 40, 80, 160, 320\} \times \sigma$, where $\sigma_{AO} = 1.6430 \text{ mJy beam}^{-1}$. Vectors denote the frequency-averaged linear polarization, with 1 mas in vector length corresponding to 4 mJy beam^{-1} .

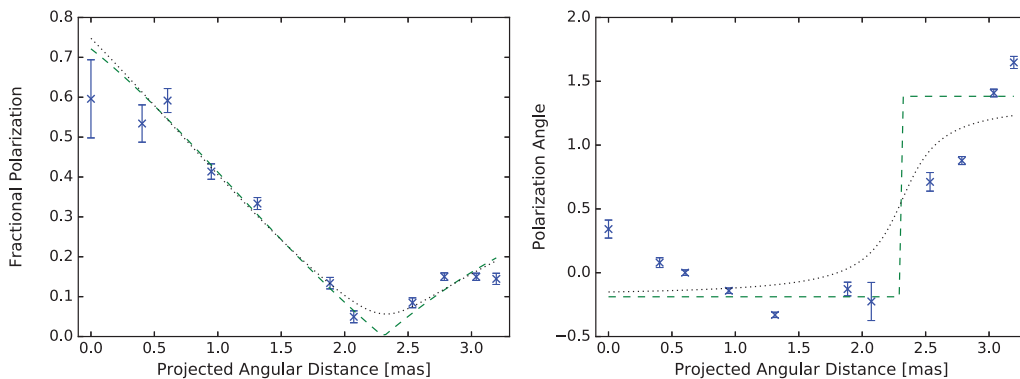


Figure 2. Fractional linear polarization (left) and relative EVPA (right) as a function of projected angular distance for epoch BD46AP. In both plots, 'X's with errors indicate the data. (Note: errors from absolute calibration of EVPA are not included, since the shape of the profile is the focus.) The best fit of the fractional linear polarization from GKK with $K = 0$ is the dashed line, while the fit with non-zero K is the dotted line.

Alternately, if the polarization is mainly governed by anisotropy of pumping radiation conditions, such a rotation could indicate a change in those conditions across the maser feature (Asensio Ramos *et al.* 2005). Here, we discuss our analysis of a maser feature with an internal EVPA rotation of $\sim \pi/2$ that persists across five epochs of observations, and our application of several tests of SiO maser polarization theories to the feature.

2. Observations

For this analysis, we used five epochs of the long-term, full-polarization SiO $\nu = 1J = 1 - 0$ (43 GHz) VLBA campaign of the Mira variable, TX Cam. These observations have been previously analyzed for total intensity and kinematics (Diamond & Kemball 2003, Gonidakis *et al.* 2010), and linear polarization (Kemball *et al.* 2009). This work

focuses on epoch codes BD46AN, BD46AO, BD46AP, BD46AQ, and BD46AR. For further information on the observations themselves, please see Diamond & Kemball (2003).

In addition, the linear polarization of our target maser feature was analyzed for one epoch (BD46AQ) in Kemball *et al.* (2011). As was done in that work, we reduce the data using the method described in Kemball & Richter (2011), to obtain accurate measurements of the low levels of circular polarization. This work in particular expands on previous work by increasing the number of epochs analyzed with accurate circular polarization and applying additional tests of maser polarization theory to the data.

3. Discussion

GKK and Linear Polarization. GKK cite an asymptotic solution for fractional Q and U polarization, Y and Z, respectively, in the regime $\Delta\omega \gg g\Omega \gg R \gg \Gamma$, as $Y = \frac{3\sin^2\theta - 2}{3\sin^2\theta}$, $Z = K$ for $\sin^2\theta \geq \frac{1}{3}$, and $Y = -1, Z = 0$ for $\sin^2\theta \leq \frac{1}{3}$, where Stokes V is assumed to be zero and K is some number such that $Y^2 + Z^2 \leq 1$. Typical applications of this theory assume $K = 0$. In the first plot in Figure 2, we fit the predicted linear polarization fraction, m_l , as a function of projected angular distance to the prediction by GKK. To do this, we assumed θ was a quadratic function of projected angular distance, d , and fit for the first- and second-order coefficients, and d_f , the value of d at which θ is the Van Vleck angle, following Kemball *et al.* (2011): $\theta = p_0(d^2 - d_f^2) + p_1(d - d_f) + \arcsin\sqrt{2/3}$. For completeness, we fit for both $K = 0$ and non-zero K . Notably, while this profile fit some epochs better than others, it provides a remarkably good fit.

The expected EVPA profiles are derived directly from the best fit functions to m_l , and then fit to the measured EVPA with a simple vertical offset, as we are not accounting for absolute EVPA. The results can be seen in the second plot in Figure 2.

In this case, $K = 0$ GKK predicts a that the EVPA profile will be a strict step function, whereas the data show a smooth rotation of the linear polarization. Generally, adding a non-zero K smooths out the rotation. However, it also causes the extremal angles to be approached asymptotically and can result in less of a net rotation. In contrast, most epochs of our data actually show a rotation of slightly more than $\pi/2$. Notably, such an investigation of EVPA rotation was also conducted by Vlemmings & Diamond (2006) for an H₂O maser of W43A, although the complex Zeeman structure of the water transition prevents the results from being directly analogous.

Zeeman Circular Polarization. Although GKK assumed Stokes $V = 0$, others have expanded on this theory by deriving the behavior of circular polarization due to Zeeman splitting. Elitzur (1996) predicted that the $m_c \propto 1/\cos\theta$. Gray (2012) predicted that m_c is roughly proportional to $\cos\theta$ but it may not be a purely linear relation. Finally, Watson & Wyld (2001) predicted a more complex, peaked function for $m_c(\cos\theta)$. The left plot in Figure 3 shows measured m_c as a function of $\cos\theta$ as determined from the $K = 0$ GKK fit to the linear polarization fraction profile. Although there is scatter at higher $\cos\theta$, our data appears most consistent with the prediction from Gray (2012).

Non-Zeeman Circular Polarization. Wiebe & Watson (1998) suggested that circular polarization may be a result of conversion from linear polarization due to non-Zeeman effects such as changing optical axes in the medium or a change in the magnetic field orientation along the line of sight. This type of non-Zeeman circular polarization would be limited by $m_c < m_l^2/4$ (Wiebe & Watson 1998). As shown in the second plot of Figure 3, the vast majority of our data are not consistent with this limit. Wiebe & Watson (1998) suggest that, individual points may fall outside this limit, but the average values should be consistent if the circular polarization is arising via this mechanism. Even averaging

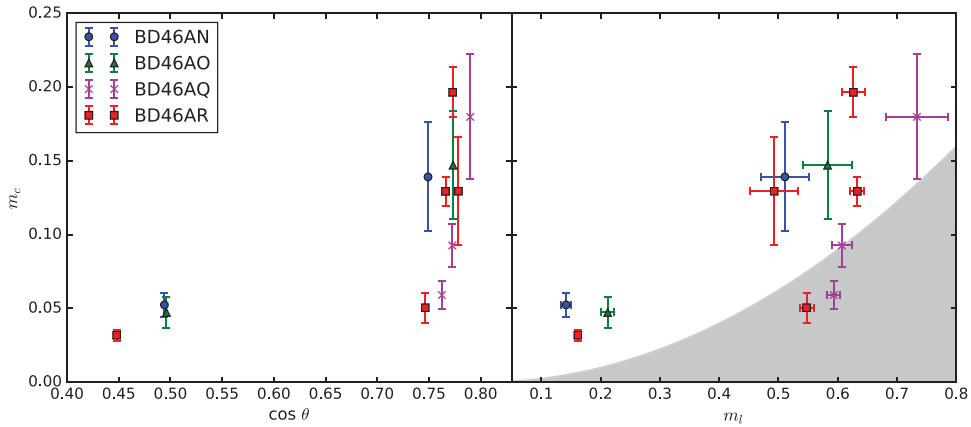


Figure 3. Fractional circular polarization, m_c , as a function of $\cos \theta$, as determined by the K=0 GKK fit (left) and fractional linear polarization, m_l (right). Points shown have m_c $S/N > 3$. Grey shading in right plot denotes region consistent with $m_c < m_l^2/4$.

our values over epoch, not a single epoch is consistent with this limit. This is consistent with the findings of Cotton *et al.* (2011).

Alternative Theories. Other explanations of this EVPA rotation include a curvature of the magnetic field itself within the masing material. Local changes in the direction of the magnetic field such as this have been predicted in Soker & Clayton (1999). In this case, the EVPA would be tracing the projected magnetic field as it rotates. However, if this was the case, we wouldn't expect to see the m_l profile that so closely resembles GKK.

Another possibility is that, instead of resulting from interaction with magnetic fields, the change in EVPA is a result of changing anisotropy conditions. Asensio Ramos *et al.* (2005) propose that a change the anisotropic pumping conditions could cause a rotation in the EVPA. However, a more extensive parameter space and lack of concurrent m_l predictions prevent application of a definitive test.

Acknowledgements

This material is based upon work supported by the National Science Foundation Graduate Research Fellowship Program under Grant No. DGE - 1144245.

References

- Asensio Ramos, A., Landi Degl'Innocenti, E., & Trujillo Bueno, J. 2005, *ApJ*, 625, 985
 Cotton, W. D., Ragland, S., & Danchi, W. C. 2011, *ApJ*, 736, 96
 Diamond, P. J. & Kemball, A. J. 2003, *ApJ*, 599, 1372
 Elitzur, M. 1996, *ApJ*, 457, 415
 Goldreich, P., Keeley, D. A., & Kwan, J. Y. 1973, *ApJ*, 179, 111.
 Gonidakis, I., Diamond, P. J., & Kemball, A. J. 2010, *MNRAS*, 406, 395
 Gray, M. 2012, *Maser Sources in Astrophysics*, (Cambridge, UK: Cambridge University Press)
 Kemball, A. J., Diamond, P. J., Gonidakis, I., *et al.* 2009, *ApJ*, 698, 1721
 Kemball, A. J., Diamond, P. J., Richter, L., Gonidakis, I., & Xue, R. 2011, *ApJ*, 743, 69
 Kemball, A. J. & Richter, L. 2011, *A&A*, 533, A26
 Soker, N. & Clayton, G. C. 1999, *MNRAS*, 307, 993
 Vlemmings, W. H. T. & Diamond, P. J. 2006, *ApJ*, 648, L59
 Watson, W. D. 2009, *RevMexAA (Serie de Conferencias)*, 36, 113
 Watson, W. D. & Wyld, H. W. 2001, *ApJ*, 558, L55
 Wiebe, D. S. & Watson, W. D. 1998, *ApJ*, 503, L71